

**substance: CrSi<sub>2</sub>**

**property: transport properties**

**resistivities**

(in 10<sup>-4</sup> Ω cm)

(see Figs. 1 and 2)

$\rho$	$\approx 10$	RT	highly degenerate p-type region	64S, 72N, 78N
	$1.9 \exp(1740/T)$	$T > 700$ K	hot-pressed bar, intrinsic region	78N
$\rho_{\parallel}$	$3.0 \exp(1850/T)$	$T > 700$ K, along [001]	intrinsic region; dc method	72N
$\rho_{\perp}$	$1.6 \exp(1850/T)$	$T > 700$ K	intrinsic region	72N

Hall effect, thermoelectric power, Nernst-Ettingshausen effect and thermal conductivity: Figs. 3...9

**carrier mobilities**

(see also Figs. 11...13)

$\mu_n$	$0.27 \text{ cm}^2/\text{V s}$	RT		73N
$\mu_p$	$8 \text{ cm}^2/\text{V s}$	RT		73N
	$7.0 \cdot 10^4 T^{-3/2}$ $\text{cm}^2/\text{V s}$	$T = 300 \dots 1200$ K	Hall mobility $R_H/\rho$	78N

**mobility ratio**

$b$	0.035 0.01	RT		73N 78N
			derived from extrinsic/ intrinsic resistivities	

**thermal conductivity**

$\kappa$	$0.071 \text{ W cm}^{-1} \text{ K}^{-1}$	RT		60N
----------	--	----	--	-----

**anisotropy of resistivity, mobility, thermoelectric power and thermal conductivity**

$\rho_{\parallel}/\rho_{\perp}$	1.9		roughly constant below 700 K, decreases at higher temperature	72N
	1.5...1.7	RT		67V

no anisotropy of the Hall coefficient at 100...500 K [70K], 85...1100 K [72N].

$S_{\parallel}/S_{\perp}$	1.7 1.3	RT	for the temperature range 100...1100 K, see Figs. 7, 8. No variation of $S_{\parallel} - S_{\perp}$ with carrier concentration for samples with $\rho = 0.09 \dots 0.3 \text{ m}\Omega \text{ cm}$ [67V].	67V
$\kappa_{\parallel}/\kappa_{\perp}$	1.2	RT	for the temperature range 300...950 K, see Fig. 10	67V

anisotropy of Hall mobility: Fig. 13, mobility ratio  $b_{\parallel} \ll b_{\perp} = 0.01$  [72N].

**hole concentration**

$p$	$6.2 \cdot 10^{20} \text{ cm}^{-3}$	$T = 85 \dots 600 \text{ K}$	from Hall effect in 0.5...6.5 kG (degenerate semiconductor)	72N
	$4 \cdot 10^{20} \text{ cm}^{-3}$	$T = 90 \dots 500 \text{ K}$ , undoped sample	from Hall effect in 5 kG, $p$ decreases with excess Si (compare Fig. 3)	64S
	$7.7 \cdot 10^{20} \text{ cm}^{-3}$	RT, pure $\text{CrSi}_2$		78N

## References:

- 60N Nikitin, E. N.: Fiz. Tverd. Tela 2 (1960) 2685 (translation: Sov. Phys. Solid State 2 (1961) 2389).
- 64S Shinoda, D., Asanabe, S., Sasaki, Y.: J. Phys. Soc. Jpn. 19 (1964) 269.
- 67V Voronov, B. K., Dudkin, L. D., Trusova, N. N.: Kristallografiya 12 (1967) 519 (translation: Sov. Phys. Cryst. 12 (1967) 448).
- 70K Kaidanov, V. I., Tselishchev, V. A., Usov, A. P., Dudkin, L. D., Voronov, B. K., Trusova, N. N.: Fiz. Tekh. Poluprovod. 4 (1970) 1338 (translation: Sov. Phys. Semicond. 4 (1971) 1135).
- 72N Nishida, I.: J. Mater. Sci. 7 (1972) 1119.
- 72V Voronov, B. K., Dudkin, L. D., Trusova, N. N.: in "Chemical Bonds in Solids" Vol. 4 (ed. N. N. Sirota) Consultants Bureau, New York 1972, 21.
- 73N Nikitin, F. N., Tarasov, V. I., Zaitsev, V. K.: Fiz. Tverd. Tela 15 (1973) 1254 (translation: Sov. Phys. Solid State 15 (1973) 846).
- 78N Nishida, I., Sakata, T.: J. Phys. Chem. Solids 39 (1978) 499.

**Fig. 1.**

$\text{CrSi}_{2+\delta}$  and  $\text{Cr}_{0.88}\text{Mn}_{0.12}\text{Si}_2$ . Resistivity vs. reciprocal temperature [64S]. 1:  $\text{CrSi}_2$  (single crystal of unknown orientation), 2:  $\text{CrSi}_{2.01}$  (polycrystalline), 3:  $\text{CrSi}_{2.02}$  (polycrystalline), 4:  $\text{Cr}_{0.88}\text{Mn}_{0.12}\text{Si}_2$  (crystal grown by the Bridgman technique).

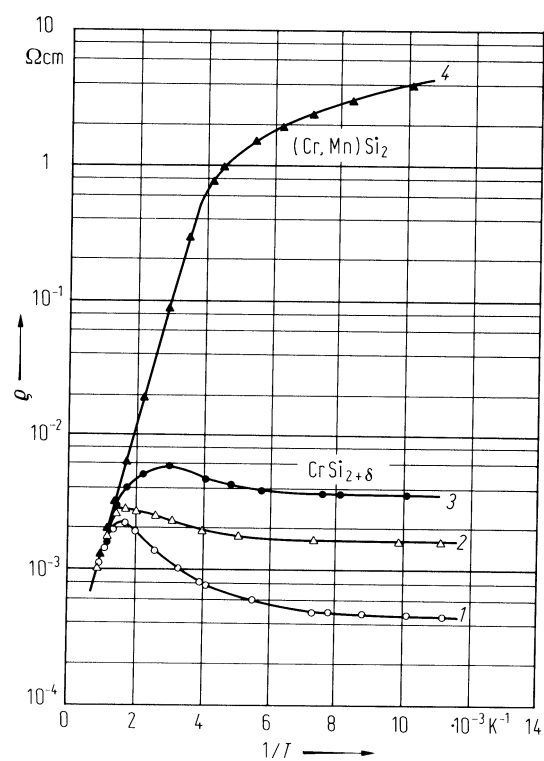


**Fig. 2.**

$\text{Cr}_{1-x}\text{Mn}_x\text{Si}_2$ . Resistivity vs. reciprocal temperature for hot-pressed samples annealed at 1373 K [78N]. Mn concentration (in parentheses) in  $10^{21} \text{ cm}^{-3}$ . 1:  $x = 0$ , 2:  $x = 0.059$  (1.65), 3:  $x = 0.100$  (2.80), 4:  $x = 0.115$  (3.23), 5:  $x = 0.142$  (3.99), 6:  $x = 0.182$  (5.12).

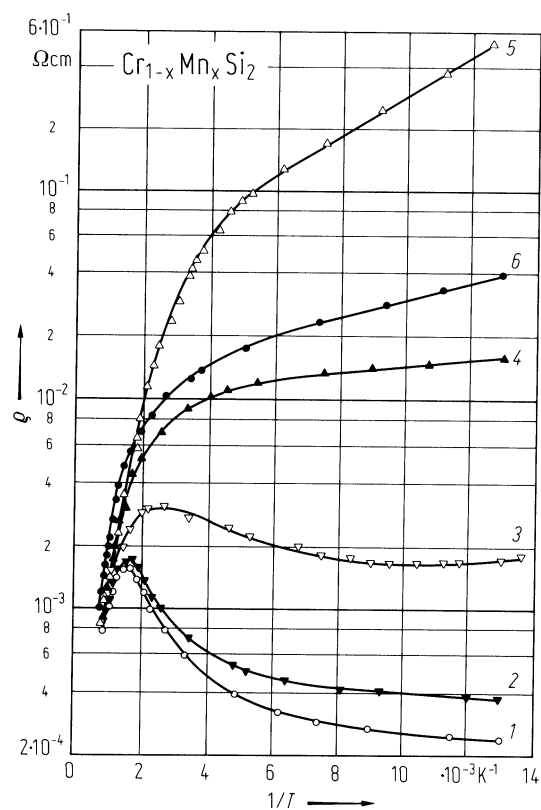


**Fig. 3.**

$\text{CrSi}_{2+\delta}$  and  $\text{Cr}_{0.88}\text{Mn}_{0.12}\text{Si}_2$ . Hall coefficient vs. reciprocal temperature [64S]. Symbols as in Fig. 1.

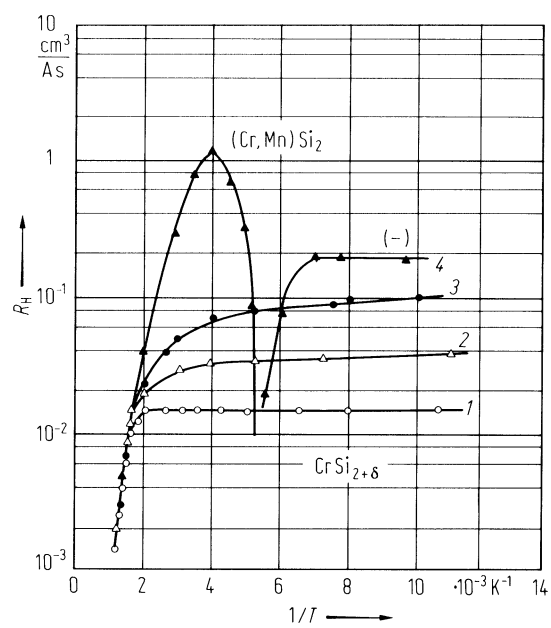


**Fig. 4.**

$\text{Cr}_{1-x}\text{Mn}_x\text{Si}_2$ . Hall coefficient vs. reciprocal temperature [78N]. Mn concentrations as in Fig. 2.

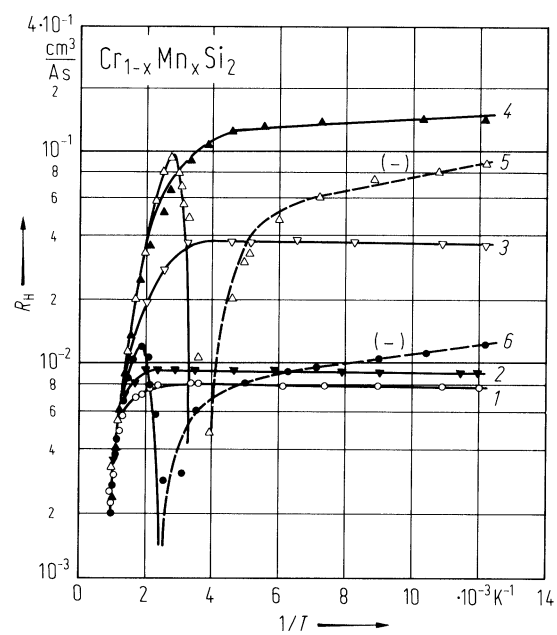


**Fig. 5.**

$\text{CrSi}_{2+\delta}$  and  $\text{Cr}_{0.88}\text{Mn}_{0.12}\text{Si}_2$ . Thermoelectric power vs. temperature [64S]. The solid curves are calculated. Symbols as in Fig. 1.

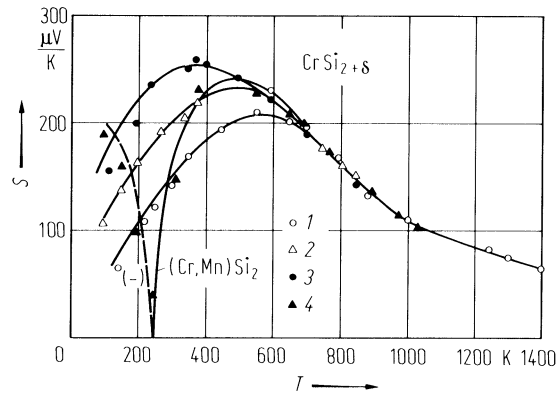




**Fig. 6.**

$\text{Cr}_{1-x}\text{Mn}_x\text{Si}_2$ . Seebeck coefficient  $S$  vs. temperature [78N]. Mn concentrations as in Fig. 2. Solid and dashed curves are calculated for acoustic lattice scattering and for impurity ion scattering, respectively.

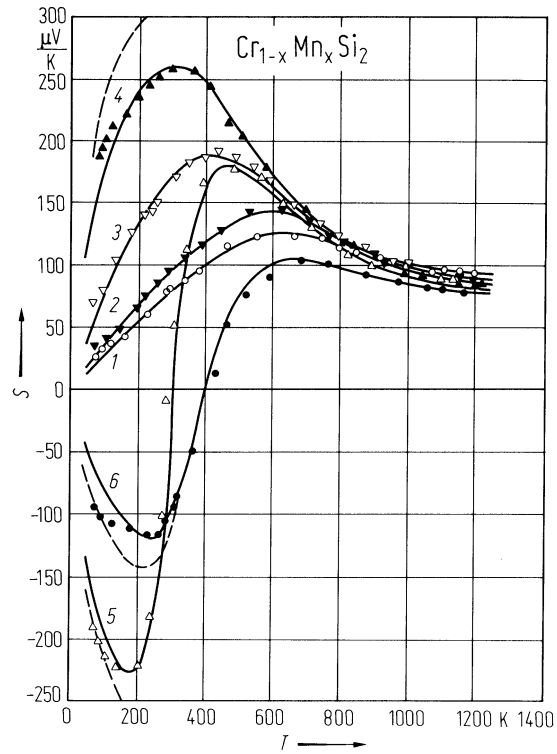


**Fig. 7.**

$\text{CrSi}_2$ . Anisotropic Seebeck coefficient vs. temperature [72N]. The solid curves are calculated with the mobility ratio  $b = 0$ , while the dotted curves are calculated with  $b = 0.01$ . Compare [72V].

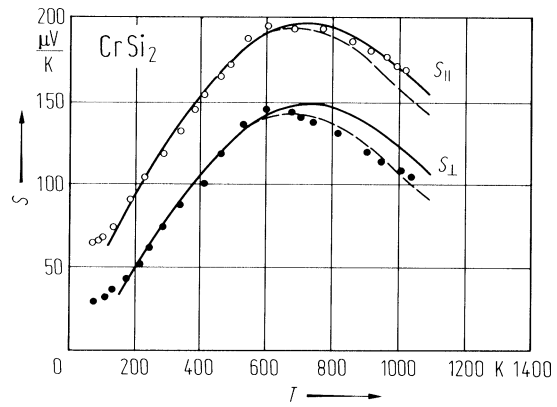


**Fig. 8.**

$\text{CrSi}_2$ . Anisotropy of the thermoelectric power vs. temperature [72N]. The sample contained 66.43 % Si.

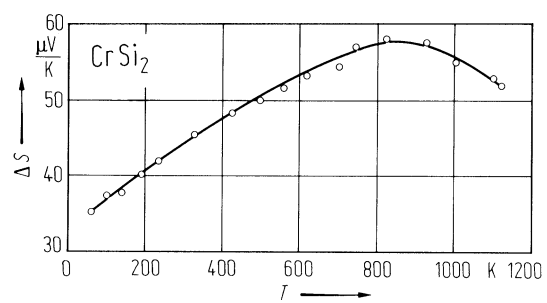


**Fig. 9.**

CrSi<sub>2</sub>. Nernst coefficient  $B$  vs. temperature [70K]. Curve 1:  $B_{aca}$ , 2:  $B_{aac}$ .

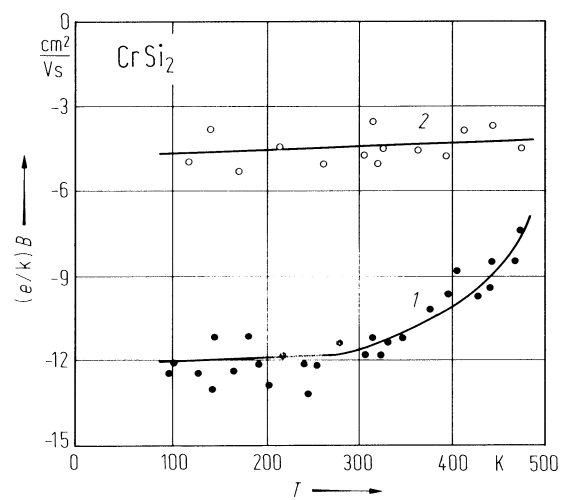


**Fig. 10.**

$\text{CrSi}_2$ . Thermal conductivity vs. temperature [72V]. Full curves: total thermal conductivity; broken curves: lattice contribution.  $\parallel$ : parallel to the  $c$  axis;  $\perp$ : perpendicular to the  $c$  axis.

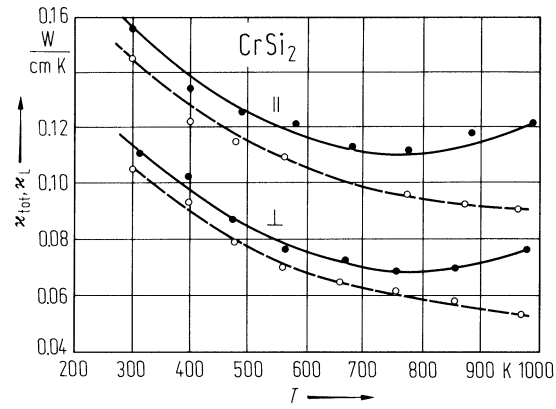


**Fig. 11.**

$\text{CrSi}_{2+\delta}$  and  $\text{Cr}_{0.88}\text{Mn}_{0.12}\text{Si}_2$ . Hall mobility of holes vs. temperature in a doubly-logarithmic scale [64S]. Symbols as in Fig. 1.

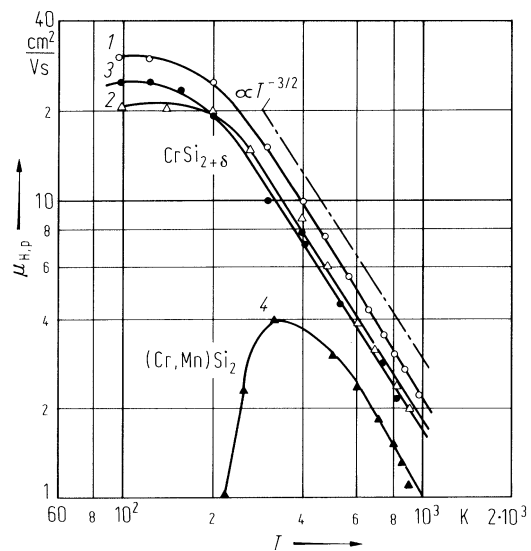


**Fig. 12.**

$\text{Cr}_{1-x}\text{Mn}_x\text{Si}_2$ . Hall mobilities vs. reciprocal temperature in a doubly-logarithmic scale [78N]. Mn concentrations as in Fig. 2. Samples are hot-pressed at 1473 K and annealed at 1373 K.

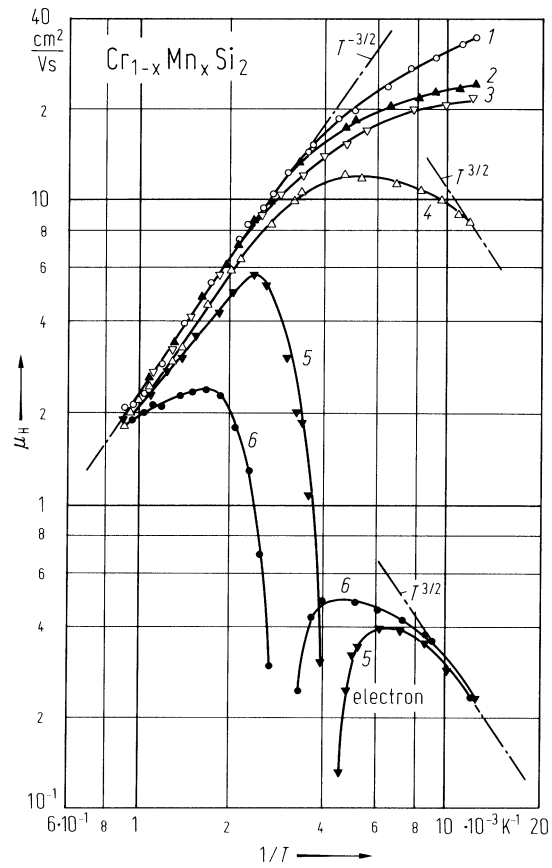


**Fig. 13.**

$\text{CrSi}_2$ . Hall mobility of holes vs. reciprocal temperature in a doubly-logarithmic scale [72N].  $\mu_{||}$ : along the  $c$  axis,  $\mu_{\perp}$ : along the  $a$  axis.

